Giant room-temperature magnetoresistance in single-crystal Fe/MgO/Fe magnetic tunnel junctions

SHINJI YUASA[1,2]*, TARO NAGAHAMA[1], AKIO FUKUSHIMA[1], YOSHISHIGE SUZUKI[1] AND KOJI ANDO[1]

[1]NanoElectronics Research Institute, National Institute of Advanced Industrial Science and Technology (AIST), Tsukuba, Ibaraki 305-8568, Japan

[2]PRESTO, Japan Science and Technology Agency, Kawaguchi, Saitama 332-0012, Japan

*e-mail: yuasa-s@aist.go.jp

Published online: 31 October 2004; doi:10.1038/nmat1257

The tunnel magnetoresistance (TMR) effect in magnetic tunnel junctions (MTJs)[1,2] is the key to developing magnetoresistive random-access-memory (MRAM), magnetic sensors and novel programmable logic devices[3–5]. Conventional MTJs with an amorphous aluminium oxide tunnel barrier, which have been extensively studied for device applications, exhibit a magnetoresistance ratio up to 70% at room temperature[6]. This low magnetoresistance seriously limits the feasibility of spintronics devices. Here, we report a giant MR ratio up to 180% at room temperature in single-crystal Fe/MgO/Fe MTJs. The origin of this enormous TMR effect is coherent spin-polarized tunnelling, where the symmetry of electron wave functions plays an important role. Moreover, we observed that their tunnel magnetoresistance oscillates as a function of tunnel barrier thickness, indicating that coherency of wave functions is conserved across the tunnel barrier. The coherent TMR effect is a key to making spintronic devices with novel quantum-mechanical functions, and to developing gigabit-scale MRAM.

The MR ratio is defined as $(R_{ap}-R_p)/R_p$, where R_p and R_{ap} are the tunnel resistance when the magnetizations of the two electrodes are aligned in parallel and antiparallel, respectively. The Fe(001)/MgO(001)/Fe(001) MTJs are theoretically expected to exhibit an extremely high MR ratio due to coherent tunnelling[7,8]. When the coherency of electron wave functions is conserved during tunnelling, only conduction electrons whose wave functions are totally symmetrical with respect to the barrier-normal axis are connected to the electronic states in the barrier region and have significant tunnelling probability. The Δ_1 band in the Fe(001) electrode has totally symmetrical characteristics. The majority spin Δ_1 band has states at the Fermi energy E_F, whereas the minority spin Δ_1 band has no states at the E_F. This makes R_{ap} much higher than R_p, resulting in the gigantic MR ratio. Fully epitaxial Fe(001)/MgO(001)/Fe(001) MTJs have been investigated experimentally[9–13], and an MR ratio of 88% has been obtained at room temperature in our previous study[13]. Although this MR ratio is the highest room-temperature value that has been reported, there has been no direct evidence that coherency of the electron wave functions is conserved across the tunnel barrier. Such conservation of coherency is essential to obtaining spintronic devices with novel quantum mechanical functions.

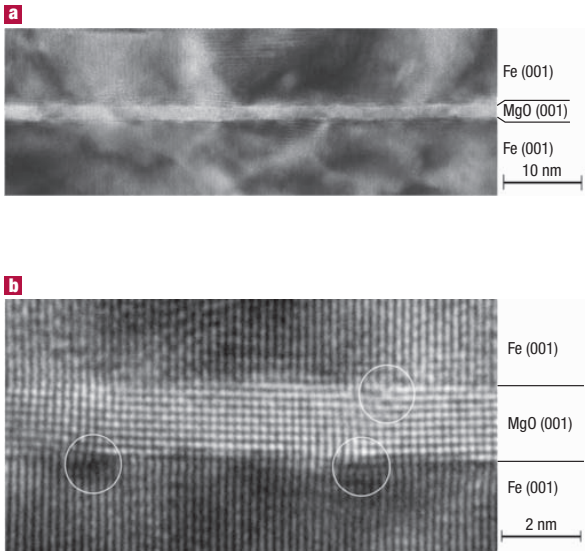


Figure 1 TEM images of a single-crystal MTJ with the Fe(001)/MgO(001)(1.8 nm)/Fe(001) structure. b is a magnification of **a**. The vertical and horizontal directions respectively correspond to the MgO[001] (Fe[001]) axis and MgO[100] (Fe[110]) axis. Lattice dislocations are circled. The lattice spacing of MgO is 0.221 nm along the [001] axis and 0.208 nm along the [100] axis. The lattice of the top Fe electrode is slightly expanded along the [110] axis.

In this study, we prepared single-crystal Fe(001)/MgO(001)/Fe(001) MTJs with MgO barrier thicknesses (t_{MgO}) from 1.2 to 3.2 nm

©2004 Nature Publishing Group

IP Bridge Exhibit 2008
Western Digital v. IP Bridge
IPR2024-01493

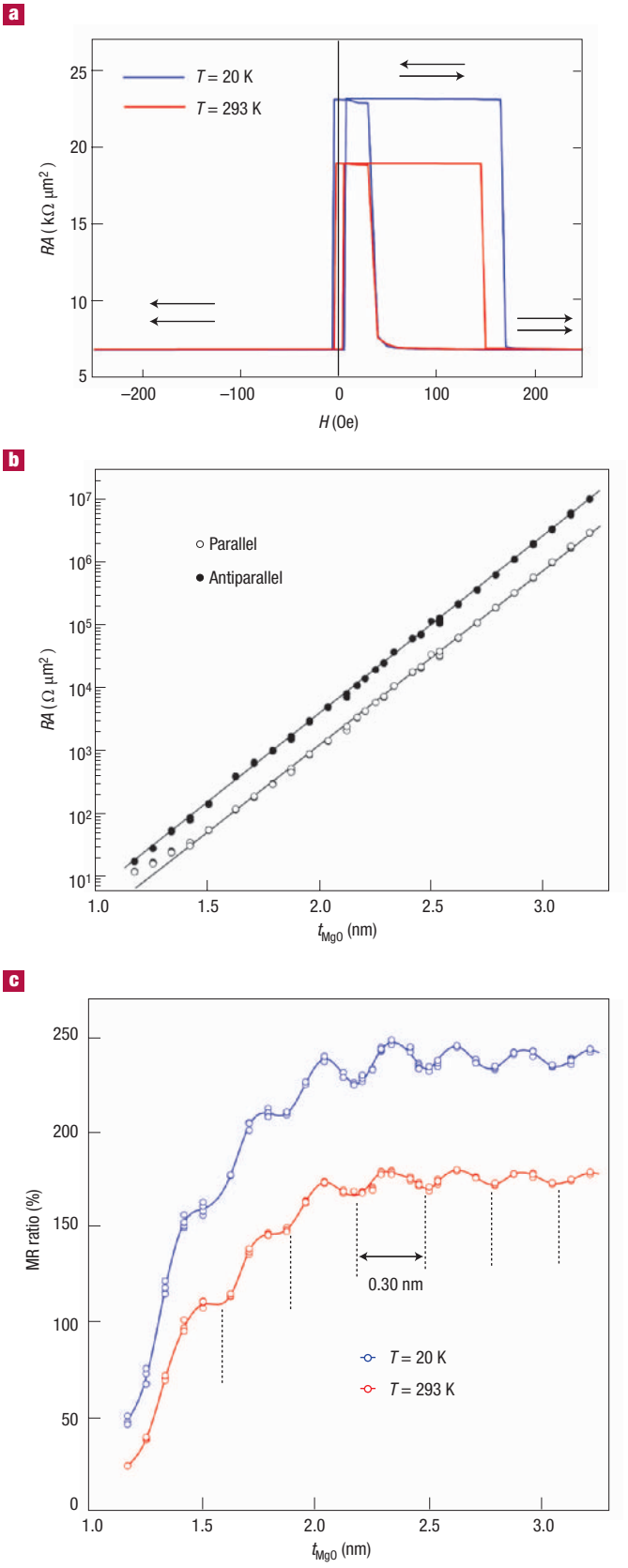


Figure 2 Tunnel magnetoresistance of Fe(001)/MgO(001)/Fe(001) junctions. **a**, Magnetoresistance curves (measured at a bias voltage of 10 mV) at $T = 293$ K and 20 K (MgO thickness $t_{MgO} = 2.3$ nm). The resistance–area product RA plotted here is the tunnel resistance for a 1×1 μm area. Arrows indicate magnetization configurations of the top and bottom Fe electrodes. The MR ratio is 180% at 293 K and 247% at 20 K. **b**, RA at $T = 20$ K (measured at a bias voltage of 10 mV) versus t_{MgO}. Open and filled circles represent parallel and antiparallel magnetic configurations. The scale of the vertical axis is logarithmic. **c**, MR ratio at $T = 293$ K and 20 K (measured at a bias voltage of 10 mV) versus t_{MgO}.

by using molecular beam epitaxy (MBE) and microfabrication techniques (see Methods). Cross-sectional transmission electron microscope (TEM; Hitachi H-9000NAR) images of an MTJ with $t_{MgO} = 1.8$ nm are shown in Fig. 1. Single-crystal lattices can be identified in the images. The lattice image for MgO(001) (Fig. 1b) illustrates that the lattice spacing is elongated along the [001] axis by 5% and is compressed along the [100] axis by 1.2% compared with the lattice of bulk MgO. Although the MgO lattice is compressed along the [100] axis to match the Fe lattice, the in-plane lattice constant of MgO is still 2.5% larger than that of bulk Fe. This lattice mismatch is relaxed by dislocations formed at the interfaces (see Fig. 1b). More dislocations are observed at the lower interface than at the upper interface. This is because the lattice of the top Fe electrode is expanded by 1.9% along the [110] axis to match the MgO lattice.

The magnetoresistance at bias voltages up to 1,300 mV was measured at 293 K and 20 K by using the d.c. four-probe method. The bias direction was defined with respect to the top Fe electrode. Typical magnetoresistance curves for the Fe/MgO/Fe/IrMn MTJ at 293 K and 20 K are shown in Fig. 2a. At 293 K the MTJ has an MR ratio of 180%, which is more than twice the highest room-temperature MR ratio reported to date[13]. Resistance of the MTJ for a 1×1 μm area (resistance–area product RA) is plotted as a function of t_{MgO} in Fig. 2b. Its exponential increase as a function of t_{MgO} is typical of ideal tunnel junctions[14]. According to the Wenzel–Kramer–Brillouin (WKB) approximation, the slope of the $\log(RA)$ versus t_{MgO} plot corresponds to $4\pi(2m\phi)^{1/2}/h$, where m, ϕ and h are, respectively, the electron mass, the potential barrier height (energy difference between the Fermi level and the bottom of the conduction band in the tunnel barrier), and Planck's constant[15]. The slope yields a barrier height ϕ of 0.39 eV. Simmons' equations for I–V characteristics[15] yield $\phi = 0.37$–0.40 eV. The barrier height of our MTJs is considerably lower than the values in the literature[9,10], which should be due to the oxygen vacancy defects in MgO (see Methods). Oxygen vacancies in MgO can form charge-neutral gap states (F-centres) about 1.2 eV below the bottom of conduction band[16], which raises the Fermi level above the vacancy states and makes the barrier height lower than 1.2 eV. It should be noted that the barrier height of an ideal MgO tunnel barrier[9] (3.7 eV) is too high for the device applications. It should also be noted that for an Al–O tunnel barrier, a lower barrier height yields a lower MR ratio[17]. It is surprising that in Fe/MgO/Fe MTJs, there is an enormous TMR effect despite the low barrier height. This is very favourable in applications because both a low RA and a high MR ratio can be achieved. Fe/MgO/Fe MTJs with RA values ranging from 300 to 10,000 Ω μm², which are desirable for MRAMs, have huge MR ratios over 150% at room temperature.

The dependence of the MR ratio on t_{MgO} gives valuable information on the physical mechanism of the TMR effect. According to theoretical calculations[7,8], the MR ratio increases with increasing t_{MgO}. This can be understood as follows. When the tunnel barrier is thick, the tunnelling current is dominated by electrons with momentum vectors normal to the barrier, because tunnelling probability decreases rapidly when the momentum vectors deviate from the barrier-normal direction.

©2004 Nature Publishing Group

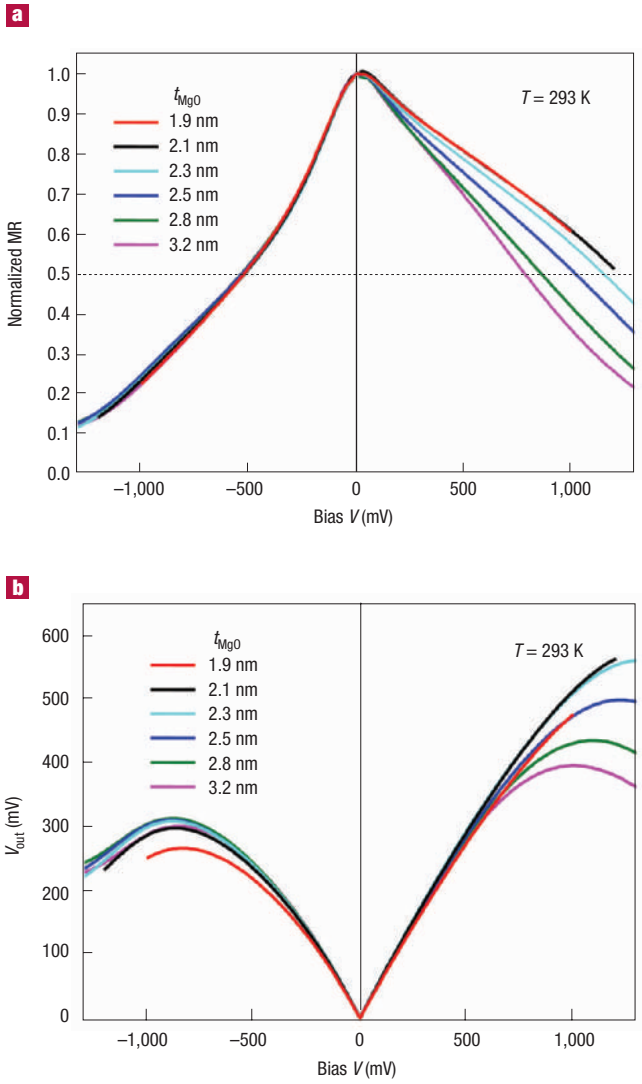


Figure 3 Bias voltage—dependence of the TMR effect. a, Relation between bias voltage V and the normalized MR ratio at room temperature of Fe(001)/MgO(001)/Fe(001) tunnel junctions with various MgO thicknesses t_{MgO}. The direction of bias voltage is defined with respect to the top electrode. **b**, Output voltage (V_{out}) of tunnel junctions, defined as $V_{out} \equiv V \times (R_{ap} - R_p)/R_{ap}$, as a function of V. Note that for positive bias the maximum V_{out} exceeds 500 mV.

The Fe-Δ_1 band has its highest spin polarization in the barrier-normal ([001]) direction, resulting in a huge MR ratio. When the tunnel barrier is thin, electrons with momentum vectors deviating from the barrier-normal direction have a finite tunnelling probability that decreases both the spin polarization and the MR ratio. The t_{MgO}-dependence of the observed MR ratio is plotted in Fig. 2c. The fact the MR ratio increases with increasing t_{MgO} agrees with the theoretical calculations. Surprisingly, the MR ratio also exhibits clear oscillatory behaviour as a function of t_{MgO}. The period of the oscillations (0.30 nm) was observed to be independent of temperature and bias voltage, but the amplitude of the oscillation decreased with increasing bias voltage. We consistently confirmed that these oscillations could be reproduced. The MR ratio for two series of MTJs separately fabricated on different substrates under the same growth conditions is shown in the Supplementary Information, Fig. S2. These two separate instances show that the TMR oscillation is very reproducible. Even MTJs prepared under different conditions, which had different MR ratios, exhibited similar TMR oscillations.

One might think that the TMR oscillation is a result of the layer-by-layer growth of MgO(001) (ref. 18), in which the growth of one monolayer is almost completed before the growth of a new monolayer begins. This could cause an oscillation in TMR because the interface morphology (atomic step density) changes periodically, layer by layer. This cannot be the origin of the observed TMR oscillations, however, because the oscillation period (0.30 nm) is not the thickness of the monoatomic MgO(001) layer (0.22 nm). A possible origin is coherent tunnelling through the MgO barrier. According to band calculations[7], there are two kinds of evanescent electronic states (Δ_1 and Δ_5 bands) at the Fermi energy in MgO. These states have complex wave vectors, the perpendicular components of which are expressed as $k_1 = k_1^r + i\kappa_1$ and $k_2 = k_2^r + i\kappa_2$. When the real parts of complex wave vectors (k_1^r and k_2^r) have different values, the tunnelling probability of electrons oscillates as a function of t_{MgO} with a period proportional to $1/(k_1^r - k_2^r)$ (ref. 7). This probability oscillation could cause an oscillation in the TMR effect. It should be noted that $(k_1^r - k_2^r)$ is a function of the in-plane components of the wave vector ($\boldsymbol{k}_{//}$). Therefore, the oscillation could not have a single oscillation period in principle. However, it is also theoretically predicted that there exists a 'hot spot' (a special point in the momentum space, where the tunnelling probability is extremely high)[7]. The oscillation therefore could have a single period for the $\boldsymbol{k}_{//}$ of a hot spot. Although the details are still to be investigated, the observed oscillation of the MR ratio should indicate that the coherency of electron wave functions is conserved across the tunnel barrier. The coherent spin-polarized tunnelling, which assures quantum mechanical correlation between wave functions in the two electrodes, is the key to achieving purely quantum-mechanical functions such as an interlayer exchange coupling across the tunnel barrier and a voltage-driven magnetization reversal[19], which will make it possible to develop spintronic devices with novel functions.

The normalized MR ratio is plotted in Fig. 3a as a function of the bias voltage (V). The asymmetrical bias-dependence evident there could be caused by asymmetric structural defects such as the dislocations at the interfaces and the lattice distortions (see Fig. 1b). The output voltage for device applications, V_{out} ($\equiv V \times (R_{ap} - R_p)/R_{ap}$), is plotted against bias voltage in Fig. 3b. It should be noted that the V_{out} at positive bias voltages can exceed 500 mV, which is nearly three times that of conventional MTJs with an Al–O barrier[20]. This high output voltage can solve problems with read-out in gigabit-scale ultrahigh-density MRAMs. Fe/MgO/Fe MTJs need not, in principle, be single-crystal devices. Even textured Fe/MgO/Fe MTJs with (001) orientation, which can be prepared on any kinds of substrates by using a highly oriented MgO(001) seed layer[21], should exhibit a similar huge TMR effect. This means that the coherent TMR effect in Fe/MgO/Fe MTJs will be a key technology in next-generation gigabit-scale MRAMs as well as in novel spintronic devices.

METHODS

Thin films for single-crystal Fe(001)/MgO(001)/Fe(001) MTJs were prepared using MBE[13,22]. A MgO(001) seed layer was first deposited on a single-crystal MgO(001) substrate to improve the morphology of the substrate surface. A 1,000-Å-thick epitaxial Fe(001) bottom electrode was then grown at room temperature and annealed at 350 °C in an ultra-high vacuum (2×10^{-8} Pa). After a reflection high-energy electron diffraction image of the Fe surface showed good crystallinity and flatness of the epitaxial Fe(001), a MgO(001) barrier layer was epitaxially grown on Fe(001) at room temperature by electron-beam evaporation of a stoichiometric MgO source material. Quadrapole mass spectroscopy revealed that the main gases in the vacuum chamber when the MgO was evaporated were O_2 and O (Supplementary Information, Fig. S1) and their partial pressures increased approximately in proportion to the rate of MgO evaporation. This indicates that some of the evaporated MgO decomposed to O atoms that formed O_2 molecules in the vacuum chamber. Because these O_2 and O gases were continuously pumped out of the vacuum chamber when the stoichiometric MgO source was evaporating, the deposited MgO film must have had some oxygen vacancy defects. The concentration of oxygen vacancies, however, was too low for them to be detected by electron probe micro-analysis (less than about 1%). To prevent the bottom Fe electrode from being oxidized, we deposited the MgO barrier layer at 0.01 nm s^{-1} under a pressure below 2.5×10^{-7} Pa. The top Fe(001) electrode (100 Å) was then

©2004 Nature Publishing Group

epitaxially grown on MgO(001) at a substrate temperature (T_S) of 200 °C. It should be noted that T_S in our previous study was room temperature[13]. The room-temperature growth of the top Fe layer resulted in higher dislocation density in the upper Fe/MgO interface. There could also be adsorbed oxygen atoms on the surface of MgO(001) after the growth of MgO. In order to obtain a clean MgO surface and to reduce the dislocation density, we grew the top Fe layer at 200 °C in this study, which actually resulted in a large enhancement of the TMR effect. A 100-Å-thick Ir-Mn antiferromagnetic layer was subsequently deposited on the Fe top electrode in order to apply an exchange bias field to the electrode. The MTJs with various MgO tunnel barrier thicknesses (t_{MgO}) were prepared on each substrate by using a combinatorial technique[22]. We deposited a wedge-shaped MgO(001) tunnel barrier layer with t_{MgO} ranging from 1.0 nm to 3.4 nm during the deposition of MgO on each 2 × 2 cm substrate. The films were then fabricated into 3 × 3 μm and 3 × 12 μm tunnel junctions by using microfabrication techniques (photolithography, Ar ion milling, and so on). We fabricated 80 MTJs on each substrate and investigated the tunnelling properties as a function of t_{MgO}. It should be noted that the variation in t_{MgO} within each MTJ is negligible because the slope of the wedge-shaped MgO layer is very small. The MTJ yield was about 95%, and the variations in the MR ratios were within ± 3% on each substrate.

Received 7 July 2004; accepted 4 October 2004; published 31 October 2004.

References

1. Moodera, J. S. *et al.* Large magnetoresistance at room temperature in ferromagnetic thin film tunnel junctions. *Phys. Rev. Lett.* **74,** 3273–3276 (1995).
2. Miyazaki, T. & Tezuka, N. Giant magnetic tunneling effect in Fe/Al_2O_3/Fe junction. *J. Magn. Magn. Mater.* **139**, L231–234 (1995).
3. Wolf, S. A. *et al.* Spintronics: A spin-based electronics vision for the future. *Science* **294,** 1488–1495 (2001).
4. Ney, A. Pampuch, C., Koch, R. & Ploog, K. H. Programmable computing with a single magnetoresistive element. *Nature* **425,** 485–487 (2003).
5. Moodera, J. S. & LeClair, P. A quantum leap. *Nature Mater.* **2,** 707–708 (2003).
6. Wang, D., Nordman, C., Daughton, J. M., Qian, Z. & Fink, J. 70% TMR at room temperature for SDT sandwich junctions with CoFeB as free and reference layers. *IEEE Trans. Magn.* **40,** 2269–2271 (2004).
7. Butler, W. H., Zhang X.-G., Schulthess, T. C. & Maclaren, J. M. Spin-dependent tunneling conductance of Fe/MgO/Fe sandwiches. *Phys. Rev. B* **63,** 054416 (2001).
8. Mathon, J. & Umerski, A. Theory of tunneling magnetoresistance of an epitaxial Fe/MgO/Fe(001) junction. *Phys. Rev. B* **63,** 220403R (2001).
9. Wulfhekel, W. *et al.* Single-crystal magnetotunnel junctions. *Appl. Phys. Lett.* **78,** 509–511 (2001).
10. Bowen, M. *et al.* Large magnetoresistance in Fe/MgO/FeCo(001) epitaxial tunnel junctions on GaAs(001). *Appl. Phys. Lett.* **79,** 1655–1657 (2001).
11. Faure-Vincent, J. *et al.* High tunnel magnetoresistance in epitaxial Fe/MgO/Fe tunnel junctions. *Appl. Phys. Lett.* **82,** 4507–4509 (2003).
12. Mitani, S., Moriyama, T. & Takanashi, K. Fe/MgO/FeCo(100) epitaxial magnetic tunnel junctions prepared by using *in situ* plasma oxidation. *J. Appl. Phys.* **93,** 8041–8043 (2003).
13. Yuasa, S., Fukushima, A., Nagahama, T., Ando, K. & Suzuki, Y. High tunnel magnetoresistance at room temperature in fully epitaxial Fe/MgO/Fe tunnel junctions due to coherent spin-polarized tunneling. *Jpn J. Appl. Phys.* **43,** L588–L590 (2004).
14. Yuasa, S. *et al.* Magnetic tunnel junctions with single-crystal electrodes: a crystal anisotropy of tunnel magneto-resistance. *Europhys. Lett.* **52,** 344–350 (2000).
15. Simmons, J. G. Electric tunnel effect between dissimilar electrodes separated by a thin insulating film. *J. Appl. Phys.* **34,** 2581–2590 (1963).
16. Gibson, A. & Haydock, R. Stability of vacancy defects in MgO: The role of charge neutrality. *Phys. Rev. B* **50,** 2582–2592 (1994).
17. Saito, Y. *et al.* Correlation between barrier width, barrier height, and dc bias voltage dependences on the magnetoresistance ratio in Ir-Mn exchange biased single and double tunnel junctions. *Jpn J. Appl. Phys.* **39,** L1035–L1038 (2000).
18. Vassent, J. L., Dynna, M., Marty, A., Gilles, B. & Patrat, G. A study on growth and the relaxation of elastic strain in MgO on Fe(001). *J. Appl. Phys.* **80,** 5727–5735 (1996).
19 You, C. Y. & Bader, S. D. Prediction of switching/rotation of the magnetization direction with applied voltage in a controllable interlayer exchange coupled system. *J. Magn. Magn. Mater.* **195,** 488–500 (1999).
20. Yu, J. H., Lee, H. M., Ando, Y. & Miyazaki, T. Electron transport properties in magnetic tunnel junctions with epitaxial NiFe (111) ferromagnetic bottom electrodes. *Appl. Phys. Lett.* **82,** 4735–4737 (2003).
21. Inaba, N. & Futamoto, M. Magnetic and crystallographic properties of Co-Cr-Pt longitudinal media prepared on MgO seedlayers deposited by ECR sputtering. *IEEE Trans. Magn.* **36,** 2372–2374 (2000).
22. Yuasa, S., Nagahama, T. & Suzuki, Y. spin-polarized resonant tunneling in magnetic tunnel junctions. *Science* **297,** 234–237 (2002).

Acknowledgements

We would like to thank M. Yamamoto, T. Katayama and Y. Yokoyama for their assistance with the experiments, and C. M. Boubeta, E. Tamura and H. Itoh for their helpful discussions.
Correspondence and requests for materials should be addressed to S.Y.
Supplementary Information accompanies the paper on www.nature.com/naturematerials.

Competing financial interests

The authors declare that they have no competing financial interests.

©2004 Nature Publishing Group